

RESEARCH

Open Access



# Microglial activation in Parkinson's disease using [<sup>18</sup>F]-FEPPA

Christine Ghadery<sup>2,3</sup>, Yuko Koshimori<sup>2,3</sup>, Sarah Coakeley<sup>2,3</sup>, Madeleine Harris<sup>2</sup>, Pablo Rusjan<sup>2</sup>, Jinhee Kim<sup>1,3</sup>, Sylvain Houle<sup>2</sup> and Antonio P. Strafella<sup>1,2,3,4\*</sup>

## Abstract

**Background:** Neuroinflammatory processes including activated microglia have been reported to play an important role in Parkinson's disease (PD). Increased expression of translocator protein (TSPO) has been observed after brain injury and inflammation in neurodegenerative diseases. Positron emission tomography (PET) radioligand targeting TSPO allows for the quantification of neuroinflammation in vivo.

**Methods:** Based on the genotype of the rs6791 polymorphism in the TSPO gene, we included 25 mixed-affinity binders (MABs) (14 PD patients and 11 age-matched healthy controls (HC)) and 27 high-affinity binders (HABs) (16 PD patients and 11 age-matched HC) to assess regional differences in the second-generation radioligand [<sup>18</sup>F]-FEPPA between PD patients and HC. FEPPA total distribution volume ( $V_T$ ) values in cortical as well as subcortical brain regions were derived from a two-tissue compartment model with arterial plasma as an input function.

**Results:** Our results revealed a significant main effect of genotype on [<sup>18</sup>F]-FEPPA  $V_T$  in every brain region, but no main effect of disease or disease × genotype interaction in any brain region. The overall percentage difference of the mean FEPPA  $V_T$  between HC-MABs and HC-HABs was 32.6% (SD = 2.09) and for PD-MABs and PD-HABs was 43.1% (SD = 1.21).

**Conclusions:** Future investigations are needed to determine the significance of [<sup>18</sup>F]-FEPPA as a biomarker of neuroinflammation as well as the importance of the rs6791 polymorphism and its clinical consequence in PD.

**Keywords:** Neuroinflammation, TSPO imaging, PET, Parkinson's disease

## Background

Parkinson's disease (PD), classically presenting with progressive motor symptoms such as tremor, rigidity, bradykinesia, and postural instability, is the second most common neurodegenerative disorder [1]. Neuroinflammatory processes including activated microglia [2, 3] as well as increased concentration of inflammatory cytokines [4–6] have been identified to play an important role in PD.

Translocator protein (TSPO), which is an 18-kDa protein located on outer mitochondrial membranes in microglia, can be found in healthy brains at very low

levels. Its increased expression has been observed in various neuropathological conditions such as amyotrophic lateral sclerosis, Alzheimer disease (AD), frontotemporal dementia, and multiple sclerosis [7].

Therefore, TSPO expression may represent a potential in vivo biomarker of neuroinflammation and reactive gliosis [8]. Positron emission tomography (PET) enables the quantification of neuroinflammation by using radioligands that target TSPO [9].

Thus far, several studies have explored the relationship between neuroinflammation and PD by using the first and most widely used radioligand [<sup>11</sup>C]-PK11195 [10, 11]. However, findings are inconclusive, and elevated TSPO binding in nigro-striatal regions have not been consistently observed [11]. This discrepancy might derive from well-known technical limitations of [<sup>11</sup>C]-PK11195 such as low signal-to-noise ratio, high nonspecific binding, low brain penetration, and high plasma protein binding [12]. As a result, second-generation TSPO radioligands such as

\* Correspondence: antonio.strafella@camh.ca; antonio.strafella@uhn.ca

<sup>1</sup>Neurology Division, Department of Medicine, Morton and Gloria Shulman Movement Disorder Unit & E.J. Safra Parkinson Disease Program, Toronto Western Hospital, UHN, University of Toronto, Ontario, Canada

<sup>2</sup>Research Imaging Centre, Campbell Family Mental Health Research Institute, Centre for Addiction and Mental Health, University of Toronto, Toronto, Ontario, Canada

Full list of author information is available at the end of the article



[<sup>18</sup>F]-FEPPA have been developed to offer a superior quality to quantify TSPO expression in vivo [13]. [<sup>18</sup>F]-FEPPA has shown a high affinity for TSPO, a suitable metabolic profile, high brain penetration, and good pharmacokinetics [14, 15].

Currently, most of the second-generation TSPO radioligands show three patterns of binding affinity based on genetic polymorphism: high-affinity binders (HABs), mixed-affinity binders (MABs), and low-affinity binders (LABs) [16]. These variations in TSPO binding affinity are derived from a single polymorphism located on exon 4 of the TSPO gene (rs6971) [17], which accounts for some of the large inter-individual variability in the outcome measures [16].

The current study represents an extension of our previous work [18] aiming to investigate whether TSPO imaging with [<sup>18</sup>F]-FEPPA using total distribution volume ( $V_T$ ) as an index of TSPO density, could be used as a potential biomarker for neuroinflammation in PD. In this study, we included a larger sample size to assess if there are regional differences in FEPPA  $V_T$  for cortical as well as subcortical brain regions between PD patients and healthy controls (HC). In addition, we are aiming to confirm our previous results by presenting potential interactions between the rs6791 polymorphism and neuroinflammation in PD.

## Methods

### Participants

Thirty patients meeting UK Brain Bank criteria for the diagnosis of idiopathic PD and 22 healthy controls participated in our study. Exclusion criteria for all participants included (1) history of a head injury, psychiatric or neurological (except PD for the patients) diseases, (2) alcohol or drug dependency or abuse, (3) contraindications for MRI scanning, and (4) use of nonsteroidal anti-inflammatory drugs. All participants were assessed for their cognitive performance using the Montreal Cognitive Assessment (MoCA) as well as their level of depression using the Beck Depression Inventory II (BDI II). For nine HC, cognitive assessment scores were only available from the Mini-Mental State Examination (MMSE). PD patients were also assessed for motor severity of the disease using the motor subset of the Unified Parkinson Disease Rating Scale (UPDRS-III). All participants underwent PET and structural MRI scans. All participants provided written informed consent following full explanation of the study procedures. The study was approved by the Centre for Addiction and Mental Health Research Ethics Board.

### PET data acquisition

A detailed description of [<sup>18</sup>F]-FEPPA synthesis was described in a previous publication [14]. It can be reliably

and quickly labeled with [<sup>18</sup>F] by nucleophilic displacement of a tosylate, leaving group in a fast one-step reaction yielding a sterile and pyrogen-free product after purification and formulation.

The PET images were obtained using a 3D High Resolution Research Tomography (HRRT) (CPS/Siemens, Knoxville, TN, USA), which measures radioactivity in 207 slices with an interslice distance of 1.22 mm. A custom-fitted thermoplastic mask was made for each participant and used with a head fixation system during the PET scans to minimize head movement (Tru-Scan Imaging, Annapolis). Following a transmission scan, intravenous [<sup>18</sup>F]-FEPPA was administered as a bolus. The scan duration was 125 min. The images were reconstructed into 34 time frames: 1 frame of variable length until the radioactivity appears in the field of view (FOV), 5 frames of 30 s, 1 frame of 45 s, 2 frames of 60 s, 1 frame of 90 s, 1 frame of 120 s, 1 frame of 210 s, and 22 frames of 300 s.

All PET images were corrected for attenuation using a single photon point source, <sup>137</sup>Cs ( $T_{50} = 30.2$  years,  $E_\gamma = 662$  keV) and were reconstructed by filtered back projection algorithm using a HANN filter at Nyquist cut-off frequency. The reconstructed image has  $256 \times 256 \times 207$  cubic voxels measuring  $1.22 \times 1.22 \times 1.22$  mm<sup>3</sup>, and the resulting reconstructed resolution is close to isotropic 4.4 mm, full width at half maximum in plane and 4.5 mm full width at half maximum axially, averaged over measurements from the center of the transaxial FOV to 10 cm off-center in 1.0-cm increments. In addition, for frame realignment for head motion correction, each image was reconstructed without attenuation correction using three iterations of iterative reconstruction [15].

### MRI acquisition

MR images for all the participants were acquired for coregistration with the corresponding PET image and the anatomical delineation of the regions of interest (ROIs). Proton density (PD)-weighted MR images were chosen for better identification of ROIs [19]. 2D oblique PD-weighted MR images were acquired with a General Electric Discovery 3.0 T MRI scanner (slice thickness = 2 mm, repetition time (TR) = 6000 ms, echo time (TE) = Min Full, flip angle = 90°, number of excitations (NEX) = 2, acquisition matrix =  $256 \times 192$ , and field of view = 22 cm).

### Input function measurement

Dispersion and metabolite-corrected plasma input function was generated as described earlier [15]. In short summary: arterial blood was taken continuously at a rate of 2.5 ml/min for the first 22.5 min after radioligand injection and the blood radioactivity levels were measured using an automatic blood sampling system (Model # PBS-101 from Veenstra Instruments, Joure, The Netherlands). In addition, 4- to 8-ml manual arterial blood samples

were obtained at 2.5, 7, 12, 15, 30, 45, 60, 90, and 120 min relative to time of injection [15]. A bi-exponential function was used to fit the blood-to-plasma ratios. A Hill function was used to fit the percentage of unmetabolized radioligand. The dispersion effect was modeled as to the convolution with a monoexponential with dispersion coefficient of 16 s and corrected with iterative deconvolution [20].

#### Generation of ROI-based time activity curve

[<sup>18</sup>F]-FEPPA PET images were preprocessed and ROIs were automatically generated using in-house software, ROMI [19]. Briefly, ROMI fits a standard template of ROIs to an individual PD-weighted MR image based on the probability of gray matter, white matter, and cerebrospinal fluid (CSF). The individual MR images are then co-registered to each summed [<sup>18</sup>F]-FEPPA PET image using the normalized mutual information algorithm so that individual refined ROI template can be transferred to the PET image space to generate the time activity curve (TAC) for each ROI. Our a priori ROIs included cortical as well as subcortical brain regions such as frontal and temporal lobes, cingulate cortex, occipital lobe, insula, hippocampus, cerebellum, thalamus, caudate nucleus, and putamen.

Dynamical series of images of [<sup>18</sup>F]-FEPPA PET were visually checked for head motion and corrected using frame-by-frame realignment. Low-noise, nonattenuation-corrected images (created with iterative reconstruction) were used to optimize the frame-by-frame realignment process. A normalized mutual information algorithm was applied with SPM8 (Wellcome Trust Centre for Neuroimaging, London, UK) to co-register each frame to the frame that showed a high signal-to-noise ratio. Parameters from the normalized mutual information were applied to the corresponding attenuation-corrected dynamic images to generate a movement-corrected dynamic image. To address the potential issues of bias from the volume loss in older participants, time activity data for all participants was corrected for the effect of partial volume error (PVE) using the Mueller-Gartner partial volume error correction algorithm as implemented in Bencherif et al. [21].

#### Kinetic analysis

$V_T$  values in each ROI were derived from a two-tissue compartment model (2-TCM) using [<sup>18</sup>F]-FEPPA radioactivity in arterial plasma as an input function and a 5% vascular contribution [15]. This method has previously been validated for [<sup>18</sup>F]-FEPPA quantification [15, 22].  $V_T$  is a ratio at equilibrium of the radioligand concentration in tissue to that in plasma (i.e., specific binding and non-displaceable uptake including non-specifically bound and free radioligand in tissue) and can be expressed in terms of kinetic rate parameters as  $V_T = K_1/k_2 (1 + k_3/k_4)$  where  $K_1$  and  $k_2$  are influx and efflux rates for radiotracer

passage across the blood-brain barrier and  $k_3$  and  $k_4$  describe the radioligand transfer between the free and non-specific compartments and the specific binding compartment. We also measured the percentage of the coefficient of variation (%COV = 100% × standard error/mean), where standard error was estimated from the diagonal of the covariance matrix of nonlinear least-squares fitting [15]. From the different ROIs, we included  $V_T$  with %COV of ≤20, which assured less data noise. Therefore, the effective sample size for each ROI varied between 34 and 52. Kinetic analyses were performed using PMOD 3.6 modeling software (PMOD Technologies Ltd., Zurich, Switzerland).

#### Voxel-based PET image analysis

For exploratory purposes, we investigated the difference between groups using voxel-based PET image analysis. Parametric images of [<sup>18</sup>F]-FEPPA  $V_T$  were generated using the Logan graphical analysis method [23]. A wavelet-based implementation of the kinetic modeling approach was applied to manage the low signal-to-noise ratio intrinsic of the voxel level quantification while maintaining the resolution [24, 25]. To examine voxel-wise group differences of  $V_T$ , an independent sample  $T$  test was conducted using Statistical Parametric Mapping (SPM12-<http://www.fil.ion.ucl.ac.uk/spm/software/spm12/>). TSPO genotype (rs6971 polymorphism) was included as a covariate. Significant level for the whole brain analysis was thresholded at  $p < 0.001$ , uncorrected.

#### DNA extraction and polymorphism genotyping

Genomic DNA was obtained from peripheral leukocytes using high salt extraction methods [26]. The polymorphism rs6971 was genotyped variously using a TaqMan1 assay on demand C\_2512465\_20 (Applied Biosystems, CA, USA). The allele T147 was linked to Vic, and the allele A147 was linked FAM. PCR reactions were performed in a 96-well microtiter-plate on a GeneAmp PCR System 9700 (Applied Biosystems, CA, USA). After PCR amplification, end point plate read and allele calling was performed using an ABI 7900 HT (Applied Biosystems, CA, USA) and the corresponding SDS software (v2.2.2). Individuals with genotype Ala147/Ala147 were classified as HABs, Ala147/Thr147 as MABs, and Thr147/Thr147 as LABs [16]. [<sup>18</sup>F]-FEPPA is not quantifiable in LABs [12]; therefore, we did not include any LAB participants in our study. Generally, LAB participants represent less than 5% in a Caucasian sample [12, 18].

#### Statistical analysis

Normality assumptions for all variables were assessed using the Kolmogorov-Smirnov test. Significant differences in means of normally distributed continuous demographical as well as clinical variables were tested by

using factorial analysis of variance (ANOVA) and independent *t* tests. If variables did not satisfy the assumption, nonparametric Mann–Whitney *U* tests and Kruskal–Wallis tests were applied. Difference in proportions was assessed by chi-square tests. To assess any sub-group differences in  $V_T$  values, we used factorial ANOVA with TSPO genotype (HAB and MAB) and disease (PD and HC) as fixed factors in cortical as well as subcortical brain regions. We controlled for injected amount by adding it as a nuisance variable in all analyses, since there was a significant difference between HC and PD. A second level of analyses was performed using the independent *t* test to compare  $V_T$  values between HC-MABs and HC-HABs as well as PD-MABs and PD-HABs. Correlations between clinical measures and  $V_T$  values were investigated in all brain regions using Pearson's correlation tests. All of the statistical analyses were performed using SPSS Statistics version 20.0. In order to establish significance, a threshold of  $p < 0.05$  was applied.

## Results

### Demographic and clinical characteristics

Demographical and clinical measures are displayed in Table 1. Based on the rs6971 polymorphism, our study sample consisted of 25 MABs with 11 HC and 14 PD patients as well as 27 HABs with 11 HC and 16 PD patients.

The factorial ANOVA showed that there were no significant differences in age as well as in specific activity at the time of injection or mass injected between MABs and HABs or between HC and PD groups. There was a

significant difference in amount injected between HC ( $M = 4.79$ ,  $SD = 0.22$ ) and PD ( $M = 5.04$ ,  $SD = 0.27$ ,  $t(50) = -3.59$ ,  $p = 0.001$ , two-tailed).

Chi-square tests showed that there were no significant differences in the composition of gender and handedness in the four groups or in the composition of symptom-dominant side between PD-MABs and PD-HABs. In addition, there were no significant differences in years of education, MoCA scores, MMSE scores, and BDI scores between MABs and HABs or between HC and PD groups. There were also no significant differences in UPDRS III, duration of disease, or total levodopa equivalent daily dose (LEDD) between PD-MABs and PD-HABs.

### Genotype and disease effects on TSPO binding

Levene's tests of equality of error variances were significant only for following regions: frontal lobe ( $p = 0.016$ ), caudate ( $p = 0.021$ ), and putamen ( $p = 0.024$ ). Therefore, we set a more stringent significance level of  $p = 0.01$  for these brain regions.

There was a significant main effect of genotype on  $V_T$  values in every brain region (Table 2) as displayed in Figs. 1, 2, and 3. There was no main effect of disease in any region of interest as well as no disease  $\times$  genotype interaction in any brain region (Table 2).

Using independent *t* tests, when comparing the effect of genotype in the HC group, HC-HABs showed significantly higher  $V_T$  values in every brain region except the cingulate, hippocampus, and thalamus compared with the HC-MAB group. Similar results were observed

**Table 1** Demographics and clinical characteristics of study participants

	Total ( $n = 52$ )	HC ( $n = 22$ )	PD ( $n = 30$ )
Age, mean (SD)	65.0 (7.70)	64.4 (8.06)	65.5 (7.54)
Gender (M:F)	33:19	11:11	22:8
TSPO genotype	27 HAB, 25 MAB	11 HAB, 11 MAB	16 HAB, 14 MAB
Handedness (R:L:both)	38:5:1	13:0:1	25:5:0
Years of education, mean (SD)	16.4 (3.25)	16.3 (3.00)	16.4 (3.40)
MoCA, median (range)	28 (26–30)	28 (26–30)	28 (26–30)
MMSE, median (range)		29.5 (27–30)	
BDI II, median (range)	6 (0–23)	4.5 (0–16)	8 (0–23)
Symptom dominant side (R:L)			19:11
UPDRS III, median (range)			24 (4–45)
Duration of disease (years), median (range)			5 (2–15)
Total LEDD, mean (SD)			395.5 (483.21)
Amount injected (mCi), mean (SD)	4.9 (0.28)	4.8 (0.22)	5.0 (0.27) <sup>a</sup>
Mass injected ( $\mu$ g), mean (SD)	1.0 (0.70)	1.1 (0.83)	1.0 (0.59)
Specific radioactivity (mCi/ $\mu$ mol), mean (SD)	2670.8 (1559.56)	2707.8 (1626.74)	2643.6 (1536.00)

Values are expressed as mean (SD) and as median (range) where applicable

UPDRS-III, Unified Parkinson's Disease Rating Scale III, MoCA Montreal Cognitive Assessment, BDI II Beck Depression Inventory II, MMSE Mini-Mental-State Examination, LEDD levodopa equivalent daily dose

<sup>a</sup>Significantly different

**Table 2** Analysis of variance of regional TSPO  $V_T$  by diagnosis and TSPO genotype

ROIs	Factorial ANOVA				Independent <i>t</i> test					
	Disease effect <sup>a</sup>		Genotype effect <sup>a</sup>		HC group			PD group		% -difference
	<i>F</i> (df)	<i>p</i>	<i>F</i> (df)	<i>p</i>	HC-MAB ( <i>n</i> = 11)	HC-HAB ( <i>n</i> = 11)	%-difference	PD-MAB ( <i>n</i> = 14)	PD-HAB ( <i>n</i> = 16)	
Frontal	$F_{(1,46)} = 0.0$	0.964	$F_{(1,46)} = 24.5$	<0.001	13.9 (2.8)	19.4 (2.8)	33.0 <sup>b</sup>	11.8 (0.2)	18.7 (1.6)	45.2 <sup>b</sup>
Temporal	$F_{(1,47)} = 0.0$	0.846	$F_{(1,47)} = 25.7$	<0.001	11.9 (2.9)	16.1 (1.8)	30.0 <sup>b</sup>	11.4 (1.2)	16.6 (1.2)	37.1 <sup>b</sup>
Cingulate	$F_{(1,35)} = 0.6$	0.427	$F_{(1,35)} = 23.0$	<0.001	9.9 (1.6)	12.3 (1.5)	21.6	8.2 (0.0)	13.7 (1.1)	50.2 <sup>b</sup>
Occipital	$F_{(1,46)} = 1.3$	0.257	$F_{(1,46)} = 21.8$	<0.001	12.3 (2.7)	17.2 (2.4)	33.2 <sup>b</sup>	13.6 (3.0)	18.3 (1.4)	29.5 <sup>b</sup>
Insula	$F_{(1,43)} = 0.1$	0.813	$F_{(1,43)} = 34.6$	<0.001	10.6 (1.8)	14.0 (1.6)	27.6 <sup>b</sup>	9.8 (0.6)	15.7 (1.3)	46.3 <sup>b</sup>
Hippocampus	$F_{(1,34)} = 0.1$	0.720	$F_{(1,34)} = 7.8$	0.009	8.7 (1.9)	10.4 (1.4)	17.8	8.6 (2.4)	12.4 (1.2)	36.2 <sup>b</sup>
Cerebellum	$F_{(1,46)} = 0.0$	0.852	$F_{(1,46)} = 34.4$	<0.001	9.6 (2.2)	14.8 (1.6)	42.6 <sup>b</sup>	9.2 (0.7)	14.7 (1.3)	46.0 <sup>b</sup>
Thalamus	$F_{(1,43)} = 0.6$	0.445	$F_{(1,43)} = 15.8$	<0.001	12.8 (3.6)	16.8 (2.6)	27.0	13.5 (2.2)	19.9 (2.0)	38.3 <sup>b</sup>
Caudate	$F_{(1,32)} = 0.0$	0.927	$F_{(1,32)} = 14.6$	0.001	8.1 (1.8)	12.4 (1.6)	41.6 <sup>b</sup>	7.2 (0.3)	12.9 (1.0)	56.7 <sup>b</sup>
Putamen	$F_{(1,41)} = 0.1$	0.717	$F_{(1,41)} = 25.9$	<0.001	8.0 (1.8)	13.5 (1.3)	51.2 <sup>b</sup>	7.8 (0.4)	12.4 (1.1)	45.5 <sup>b</sup>

Values are expressed as mean (SD). HAB, high affinity binders and MAB, mixed affinity binders refer to the single nucleotide polymorphism rs6971 of the TSPO gene known to influence [<sup>18</sup>F]-FEPPA binding. Percentage differences of the mean  $V_T$  values between HC-HABs and HC-MABs as well as PD-MABs and PD-HABs

<sup>a</sup>Main effect of univariate ANOVA

<sup>b</sup>Significantly different

among the PD group, whereas PD-HABs showed significantly higher  $V_T$  values in every brain region compared to PD-MABs ( $p < 0.05$ ).

The percentage differences of the mean  $V_T$  values between HC-MABs and HC-HABs as well as PD-MABs and PD-HABs for each brain region are displayed in Table 2. The overall percentage difference of the mean FEPPA  $V_T$  between HC-MABs and HC-HABs was 32.6% (SD = 2.09) and for PD-MABs and PD-HABs was 43.1% (SD = 1.21).

There was no correlation between LEDD, UPDRS scores, and duration of disease with  $V_T$  values in any brain region in either PD-MABs or PD-HABs.

As an additional analysis, we also evaluated our data without PVE correction to identify any changes in the results. The main results were confirmed by showing no main effect of disease, or disease × genotype interaction as well as a main effect of genotype on  $V_T$  values (data not shown).

**Voxel-based PET image analysis**

In accordance with the results of the ROI analysis, we did not find any significant difference between HC and PD groups, even when using an uncorrected threshold of  $p < 0.001$ .

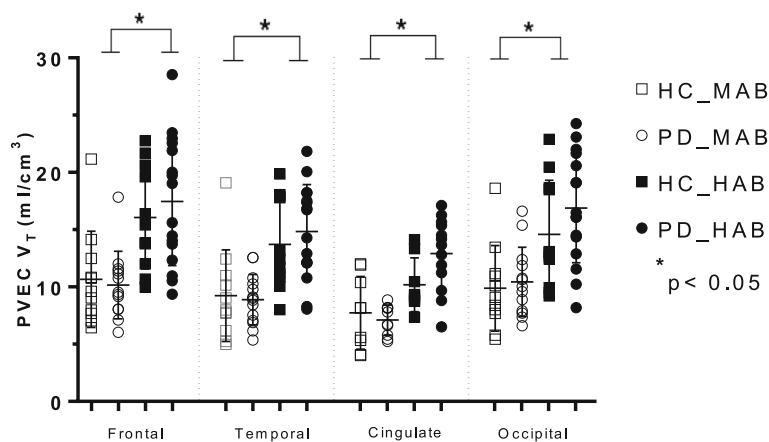


**Fig. 1** Graphs of partial volume effect corrected (PVEC) total distribution volume ( $V_T$ ) in different brain regions. Healthy control with mixed affinity binder (HC-MAB) and healthy control with high affinity binder (HC-HAB) groups as well as Parkinson's disease with mixed affinity binder (PD-MAB) and Parkinson's disease with high affinity binder (PD-HAB) groups. Asterisks indicate that the HAB groups show significantly higher  $V_T$  mean values compared with the MAB groups



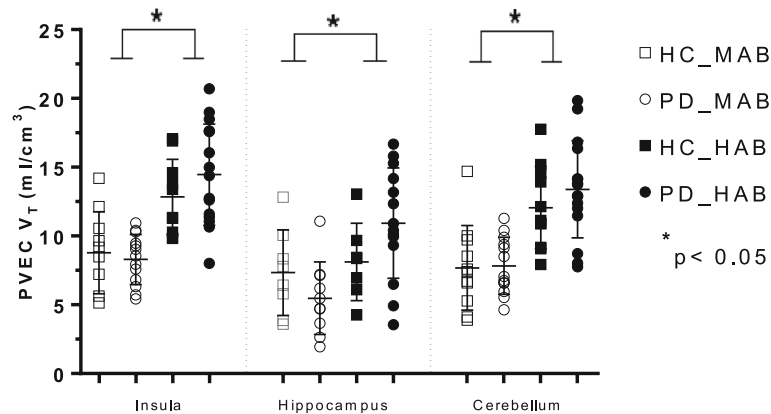


**Fig. 2** Graphs of partial volume effect corrected (PVEC) total distribution volume ( $V_T$ ) in different brain regions. Healthy control with mixed affinity binder (HC-MAB) and healthy control with high affinity binder (HC-HAB) groups as well as Parkinson’s disease with mixed affinity binder (PD-MAB) and Parkinson’s disease with high affinity binder (PD-HAB) groups. Asterisks indicate that the HAB groups show significantly higher  $V_T$  mean values compared with the MAB groups

**Discussion**

This study represents an extension of our previous work investigating the potential use of [<sup>18</sup>F]-FEPPA as a new radioligand to measure neuroinflammation in PD patients. As previously reported [12, 18], we were able to observe an influence of the rs6971 polymorphism on TSPO binding affinity. Our results showed a trend towards elevated TSPO binding, especially in the PD-HAB group by showing significantly higher  $V_T$  values in every brain region compared to PD-MABs.  $V_T$  value comparisons between HC-HABs and HC-MABs were less consistent, by showing no significant  $V_T$  value differences in some subcortical and cortical brain regions. The trend towards elevated TSPO binding, particularly in PD-HABs was also previously observed in the striatum [18].

Currently, our results indicate interactions between the rs6971 polymorphism and neuroinflammation in PD. As mentioned earlier, TSPO expression may represent a potential in vivo biomarker of neuroinflammation. Increased TSPO expression has been observed after brain injury and inflammation in neurodegenerative diseases [7, 10, 27–29]. Earlier studies have proposed a connection between the rs6971 polymorphism and variations in pregnenolone production and plasma levels of low-density lipoprotein cholesterol [30], as well as anxiety in depressive individuals [31]. So far, the functional significance of the upregulated TSPO expression is still under investigation [9]. Besides its role as a potential biomarker for neuroinflammation, TSPO has many physiological functions such as its participation in cell growth and proliferation [32] and steroidogenesis

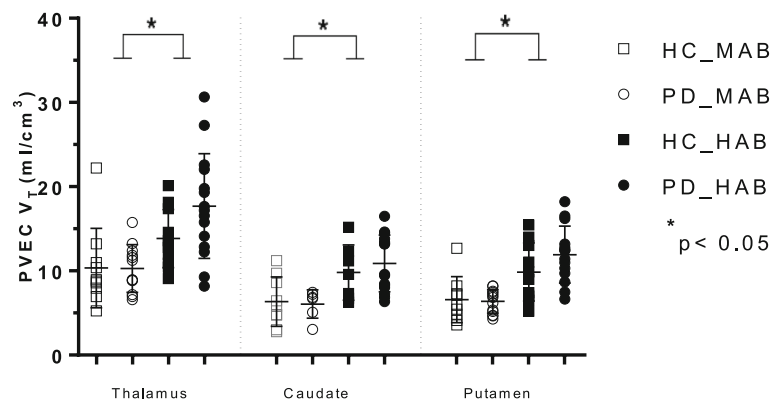


**Fig. 3** Graphs of partial volume effect corrected (PVEC) total distribution volume ( $V_T$ ) in different brain regions. Healthy control with mixed affinity binder (HC-MAB) and healthy control with high affinity binder (HC-HAB) groups as well as Parkinson’s disease with mixed affinity binder (PD-MAB) and Parkinson’s disease with high affinity binder (PD-HAB) groups. Asterisks indicate that the HAB groups show significantly higher  $V_T$  mean values compared with the MAB groups

[33], as well as in mitochondrial respiration and apoptosis [34]. Therefore, elevated TSPO levels in microglia and astrocytes may possibly increase neurosteroid synthesis at injury sites to stimulate neurotropic and neuroprotective activity [35]. Processes such as glial proliferation, migration, and phagocytosis or secretion of inflammatory cytokines in response to brain injury might be explanations for TSPO upregulation [35]. Nonetheless, since the genetic variability is present in healthy as well as in disease-affected brains, it cannot be associated with a specific neurological condition [12, 36]. However, previous investigations using second-generation TSPO radioligands have also presented a stronger disease effect on TSPO expression in AD patients [37]. Future investigations are needed to further determine the importance of this polymorphism and its clinical significance in PD.

Based on previous imaging studies from our lab [12, 38] and based on the mean and variability of  $V_T$  in our data (as displayed in Table 2), we used the *F*-test ANOVA to calculate the required total sample size, 52 participants will be needed to detect 30% difference between groups, assuming effect size  $d = 0.4$ ,  $\alpha = 0.05$  and power = 0.8.

We were not able to show a significant main effect of disease on TSPO expression in any brain region. To date, several studies have investigated the association between neuroinflammation in PD using [ $^{11}\text{C}$ ]-PK11195 PET [10, 11, 29, 39–42]. The results have been inconclusive, as some studies were able to show increased neuroinflammation in PD patients compared to HC [10, 29, 39] and others not [11, 40]. This discrepancy might be explainable by the low specific to non-specific ratio of [ $^{11}\text{C}$ ]-PK11195 [12] and methodological differences. A recent study using [ $^{11}\text{C}$ ]-DPA713 PET revealed an extrastriatal spreading of microglial activation in a small sample of PD patients [43].

In our study, we used [ $^{18}\text{F}$ ]-FEPPA, a novel radioligand exhibiting optimal chemical, pharmacokinetic, and pharmacodynamic properties for applications in imaging TSPO [22]. Our previous results could not detect any significant disease effect on [ $^{18}\text{F}$ ]-FEPPA  $V_T$  in the striatum [18]. In our current investigation, we were not able to show any anatomically widespread microglial activation in Parkinson disease, as previously observed using [ $^{11}\text{C}$ ]-PK11195 [29]. To this point, several studies observed a significant increase in [ $^{18}\text{F}$ ]-FEPPA  $V_T$  in people with major depressive episodes [44] as well as AD patients [45]. Especially in AD patients, a widespread distribution of activated microglia was noticed in gray and white matter indicating an important role of neuroinflammation in cognitive decline [45]. In addition, several studies [41, 42] including more severe cases of PD patients with dementia were able to show neuroinflammation in primarily cortical regions. Since our study

sample consisted of cognitive normal PD patients a significant disease effect might be detectable in more cognitively impaired patients.

We did not find any correlation between anti-parkinsonian medication, disease severity and duration, and [ $^{18}\text{F}$ ]-FEPPA  $V_T$ . Similar observations were detected in longitudinal data [29], showing no correlation between levels of microglial activation and clinical severity as well as disease duration. The authors of this study suggest that microglia are activated early in the disease process, but remain relatively static over a 2-year time interval. Further, in consistency with previous results [18, 46] using the same radioligand, we did not observe any age-related increase in TSPO density (data not shown).

## Conclusions

In conclusion, more studies are needed to determine the significance of [ $^{18}\text{F}$ ]-FEPPA as a biomarker of neuroinflammation in PD and to further explore its capacity to differentiate between PD patients with cognitive impairment or even dementia.

## Abbreviations

2-TCM: Two-tissue compartment model; AD: Alzheimer disease; ANOVA: Analysis of variance; BDI: Beck Depression Inventory; COV: Coefficient of variation; CSF: Cerebrospinal fluid; FOV: Field of view; HAB: High-affinity binder; HC: Healthy control; HRRT: High Resolution Research Tomography; LAB: Low-affinity binder; LEDD: Levodopa equivalent daily dose; MAB: Mixed-affinity binder; MMSE: Mini-Mental State Examination; MoCa: Montreal Cognitive Assessment; NEX: Number of excitations; PD: Parkinson's disease; PD-weighted: Proton density-weighted; PET: Positron emission tomography; PVE: Partial volume error; PVEC: Partial volume error correction; ROI: Region of interest; SD: Standard deviation; TAC: Time activity curve; TE: Echo time; TR: Repetition time; TSPO: Translocator protein; UPDRS: Unified Parkinson Disease Rating Scale;  $V_T$ : Total distribution volume

## Acknowledgements

Not applicable.

## Funding

This study was supported by the Canadian Institutes of Health Research (INE 117891). APS is supported by the Canada Research Chair program from the Canadian Institutes of Health Research.

## Availability of data and materials

The authors can confirm that all relevant data generated or analyzed during this study are included in the article and/or its supplementary information files.

## Authors' contributions

CG, YK, APS designed the study. APS and SH supervised the project. CG, YK, SC, MH collected the data. CG, YK, PR, JK analyzed the data. All authors interpreted the data. CG wrote the manuscript. All authors reviewed and edited the manuscript. All authors read and approved the final manuscript.

## Competing interests

The authors declare that they have no competing interests.

## Consent for publication

Not applicable.

## Ethics approval and consent to participate

All participants provided written informed consent following full explanation of the study procedures. The study was approved by the Centre for Addiction and Mental Health Research Ethics Board.

**Author details**

<sup>1</sup>Neurology Division, Department of Medicine, Morton and Gloria Shulman Movement Disorder Unit & E.J. Safra Parkinson Disease Program, Toronto Western Hospital, UHN, University of Toronto, Ontario, Canada. <sup>2</sup>Research Imaging Centre, Campbell Family Mental Health Research Institute, Centre for Addiction and Mental Health, University of Toronto, Toronto, Ontario, Canada. <sup>3</sup>Division of Brain, Imaging and Behaviour – Systems Neuroscience, Krembil Research Institute, UHN, University of Toronto, Ontario, Canada. <sup>4</sup>Toronto Western Hospital and Institute, CAMH-Research Imaging Centre, University of Toronto, Toronto, Ontario M5T 2S8, Canada.

Received: 7 September 2016 Accepted: 13 December 2016

Published online: 11 January 2017

**References**

- Tanner CM, Goldman SM. Epidemiology of Parkinson's disease. *Neurol Clin*. 1996;14(2):317–35.
- McGeer PL, Itagaki S, Boyes BE, McGeer EG. Reactive microglia are positive for HLA-DR in the substantia nigra of Parkinson's and Alzheimer's disease brains. *Neurology*. 1988;38(8):1285–91.
- Imamura K, Hishikawa N, Sawada M, Nagatsu T, Yoshida M, Hashizume Y. Distribution of major histocompatibility complex class II-positive microglia and cytokine profile of Parkinson's disease brains. *Acta Neuropathol*. 2003;106(6):518–26.
- Mogi M, Harada M, Kondo T, Riederer P, Inagaki H, Minami M, Nagatsu T. Interleukin-1 beta, interleukin-6, epidermal growth factor and transforming growth factor-alpha are elevated in the brain from parkinsonian patients. *Neurosci Lett*. 1994;180(2):147–50.
- Dobbs RJ, Charlett A, Purkiss AG, Dobbs SM, Weller C, Peterson DW. Association of circulating TNF-alpha and IL-6 with ageing and parkinsonism. *Acta Neurol Scand*. 1999;100(1):34–41.
- Blum-Degen D, Muller T, Kuhn W, Gerlach M, Przuntek H, Riederer P. Interleukin-1 beta and interleukin-6 are elevated in the cerebrospinal fluid of Alzheimer's and de novo Parkinson's disease patients. *Neurosci Lett*. 1995;202(1–2):17–20.
- Venneti S, Lopresti BJ, Wiley CA. Molecular imaging of microglia/macrophages in the brain. *Glia*. 2013;61(1):10–23.
- Rupprecht R, Papadopoulos V, Rammes G, Baghai TC, Fan J, Akula N, Groyer G, Adams D, Schumacher M. Translocator protein (18 kDa) (TSPO) as a therapeutic target for neurological and psychiatric disorders. *Nat Rev Drug Discov*. 2010;9(12):971–88.
- Chen MK, Guilarte TR. Translocator protein 18 kDa (TSPO): molecular sensor of brain injury and repair. *Pharmacol Ther*. 2008;118(1):1–17.
- Ouchi Y, Yoshikawa E, Sekine Y, Futatsubashi M, Kanno T, Ogusu T, Torizuka T. Microglial activation and dopamine terminal loss in early Parkinson's disease. *Ann Neurol*. 2005;57(2):168–75.
- Kobylecki C, Counsell SJ, Cabanel N, Wachter T, Turkheimer FE, Eggert K, Oertel W, Brooks DJ, Gerhard A. Diffusion-weighted imaging and its relationship to microglial activation in parkinsonian syndromes. *Parkinsonism Relat Disord*. 2013;19(5):527–32.
- Mizrahi R, Rusjan PM, Kennedy J, Pollock B, Mulsant B, Suridjan I, De Luca V, Wilson AA, Houle S. Translocator protein (18 kDa) polymorphism (rs6971) explains in-vivo brain binding affinity of the PET radioligand [(18)F]-FEPPA. *J Cereb Blood Flow Metab*. 2012;32(6):968–72.
- Chauveau F, Boutin H, Van Camp N, Dolle F, Tavtitan B. Nuclear imaging of neuroinflammation: a comprehensive review of [11C]PK11195 challengers. *Eur J Nucl Med Mol Imaging*. 2008;35(12):2304–19.
- Wilson AA, Garcia A, Parkes J, McCormick P, Stephenson KA, Houle S, Vasdev N. Radiosynthesis and initial evaluation of [18F]-FEPPA for PET imaging of peripheral benzodiazepine receptors. *Nucl Med Biol*. 2008;35(3):305–14.
- Rusjan PM, Wilson AA, Bloomfield PM, Vitcu I, Meyer JH, Houle S, Mizrahi R. Quantitation of translocator protein binding in human brain with the novel radioligand [18F]-FEPPA and positron emission tomography. *J Cereb Blood Flow Metab*. 2011;31(8):1807–16.
- Owen DR, Yeo AJ, Gunn RN, Song K, Wadsworth G, Lewis A, Rhodes C, Pulford DJ, Bennacef I, Parker CA, StJean PL, Cardon LR, Mooser VE, Matthews PM, Rabiner EA, Rubio JP. An 18-kDa translocator protein (TSPO) polymorphism explains differences in binding affinity of the PET radioligand PBR28. *J Cereb Blood Flow Metab*. 2012;32(1):1–5.
- Owen DR, Howell OW, Tang SP, Wells LA, Bennacef I, Bergstrom M, Gunn RN, Rabiner EA, Wilkins MR, Reynolds R, Matthews PM, Parker CA. Two binding sites for [3H]PBR28 in human brain: implications for TSPO PET imaging of neuroinflammation. *J Cereb Blood Flow Metab*. 2010;30(9):1608–18.
- Koshimori Y, Ko JH, Mizrahi R, Rusjan P, Mabrouk R, Jacobs MF, Christopher L, Hamani C, Lang AE, Wilson AA, Houle S, Strafella AP. Imaging striatal microglial activation in patients with Parkinson's disease. *PLoS One*. 2015;10(9):e0138721.
- Rusjan P, Mamo D, Ginovart N, Hussey D, Vitcu I, Yasuno F, Tetsuya S, Houle S, Kapur S. An automated method for the extraction of regional data from PET images. *Psychiatry Res*. 2006;147(1):79–89.
- Rusjan PM, Wilson AA, Miller L, Fan I, Mizrahi R, Houle S, Vasdev N, Meyer JH. Kinetic modeling of the monoamine oxidase B radioligand [(1)1C]SL25.1188 in human brain with high-resolution positron emission tomography. *J Cereb Blood Flow Metab*. 2014;34(5):883–9.
- Bencherif B, Stumpf MJ, Links JM, Frost JJ. Application of MRI-based partial-volume correction to the analysis of PET images of mu-opioid receptors using statistical parametric mapping. *J Nucl Med*. 2004;45(3):402–8.
- Kenk M, Selvanathan T, Rao N, Suridjan I, Rusjan P, Remington G, Meyer JH, Wilson AA, Houle S, Mizrahi R. Imaging neuroinflammation in gray and white matter in schizophrenia: an in-vivo PET study with [18F]-FEPPA. *Schizophr Bull*. 2015;41(1):85–93.
- Logan J, Fowler JS, Volkow ND, Wolf AP, Dewey SL, Schlyer DJ, MacGregor RR, Hitzemann R, Bendriem B, Gatley SJ. Graphical analysis of reversible radioligand binding from time-activity measurements applied to [N-11C-methyl]-(-)-cocaine PET studies in human subjects. *J Cereb Blood Flow Metab*. 1990;10(5):740–7.
- Rusjan P, Meyer J, Bloomfield P, Houle S. "Parametric modeling of [11C]harmine acquired on the HRRT PET," 2009. [http://jnumedmtg.snmjournals.org/cgi/content/meeting\\_abstract/50/2\\_MeetingAbstracts/1417](http://jnumedmtg.snmjournals.org/cgi/content/meeting_abstract/50/2_MeetingAbstracts/1417).
- Turkheimer FE, Brett M, Aston JA, Leff AP, Sargent PA, Wise RJ, Grasby PM, Cunningham VJ. Statistical modeling of positron emission tomography images in wavelet space. *J Cereb Blood Flow Metab*. 2000;20(11):1610–8.
- Lahiri DK, Nurnberger Jr JI. A rapid non-enzymatic method for the preparation of HMW DNA from blood for RFLP studies. *Nucleic Acids Res*. 1991;19(19):5444.
- Gerhard A, Banati RB, Goerres GB, Cagnin A, Myers R, Gunn RN, Turkheimer F, Good CD, Mathias CJ, Quinn N, Schwarz J, Brooks DJ. 11C(R)-PK11195 PET imaging of microglial activation in multiple system atrophy. *Neurology*. 2003;61(5):686–9.
- Gerhard A, Schwarz J, Myers R, Wise R, Banati RB. Evolution of microglial activation in patients after ischemic stroke: a [11C](R)-PK11195 PET study. *Neuroimage*. 2005;24(2):591–5.
- Gerhard A, Pavese N, Hotton G, Turkheimer F, Es M, Hammers A, Eggert K, Oertel W, Banati RB, Brooks DJ. In vivo imaging of microglial activation with [11C](R)-PK11195 PET in idiopathic Parkinson's disease. *Neurobiol Dis*. 2006;21(2):404–12.
- Costa B, Pini S, Gabelloni P, Da Pozzo E, Abelli M, Lari L, Preve M, Lucacchini A, Cassano GB, Martini C. The spontaneous Ala147Thr amino acid substitution within the translocator protein influences pregnenolone production in lymphomonocytes of healthy individuals. *Endocrinology*. 2009;150(12):5438–45.
- Costa B, Pini S, Martini C, Abelli M, Gabelloni P, Landi S, Muti M, Gesi C, Lari L, Cardini A, Galderisi S, Mucci A, Lucacchini A, Cassano GB. Ala147Thr substitution in translocator protein is associated with adult separation anxiety in patients with depression. *Psychiatr Genet*. 2009;19(2):110–1.
- Lee DH, Kang SK, Lee RH, Ryu JM, Park HY, Choi HS, Bae YC, Suh KT, Kim YK, Jung JS. Effects of peripheral benzodiazepine receptor ligands on proliferation and differentiation of human mesenchymal stem cells. *J Cell Physiol*. 2004;198(1):91–9.
- Papadopoulos V, Mukhin AG, Costa E, Krueger KE. The peripheral-type benzodiazepine receptor is functionally linked to Leydig cell steroidogenesis. *J Biol Chem*. 1990;265(7):3772–9.
- Casellas P, Galieue S, Basile AS. Peripheral benzodiazepine receptors and mitochondrial function. *Neurochem Int*. 2002;40(6):475–86.
- Streit WJ. Microglial response to brain injury: a brief synopsis. *Toxicol Pathol*. 2000;28(1):28–30.
- Owen DR, Gunn RN, Rabiner EA, Bennacef I, Fujita M, Kreis WC, Innis RB, Pike WW, Reynolds R, Matthews PM, Parker CA. Mixed-affinity binding in humans with 18-kDa translocator protein ligands. *J Nucl Med*. 2011;52(1):24–32.



37. Varrone A, Oikonen V, Forsberg A, Joutsa J, Takano A, Solin O, Haaparanta-Solin M, Nag S, Nakao R, Al-Tawil N, Wells LA, Rabiner EA, Valencia R, Schultze-Mosgau M, Thiele A, Vollmer S, Dyrks T, Lehmann L, Heinrich T, Hoffmann A, Nordberg A, Halldin C, Rinne JO. "Positron emission tomography imaging of the 18-kDa translocator protein (TSPO) with [18F]FEMPA in Alzheimer's disease patients and control subjects." *Eur J Nucl Med Mol Imaging*. 2015;42(3):438–46.
38. Suridjan I, Rusjan PM, Kenk M, Verhoeff NP, Voineskos AN, Rotenberg D, Wilson AA, Meyer JH, Houle S, Mizrahi R. Quantitative imaging of neuroinflammation in human white matter: a positron emission tomography study with translocator protein 18 kDa radioligand, [18F]-FEPPA. *Synapse* (New York, NY). 2014;68(11):536–47.
39. Iannaccone S, Cerami C, Alessio M, Garibotto V, Panzacchi A, Olivieri S, Gelsomino G, Moresco RM, Perani D. In vivo microglia activation in very early dementia with Lewy bodies, comparison with Parkinson's disease. *Parkinsonism Relat Disord*. 2013;19(1):47–52.
40. Bartels AL, Willemsen AT, Doorduyn J, de Vries EF, Dierckx RA, Leenders KL. [11C]-PK11195 PET: quantification of neuroinflammation and a monitor of anti-inflammatory treatment in Parkinson's disease? *Parkinsonism Relat Disord*. 2010;16(1):57–9.
41. Edison P, Ahmed I, Fan Z, Hinz R, Gelosa G, Ray Chaudhuri K, Walker Z, Turkheimer FE, Brooks DJ. Microglia, amyloid, and glucose metabolism in Parkinson's disease with and without dementia. *Neuropsychopharmacology*. 2013;38(6):938–49.
42. Fan J, Lindemann P, Feuilleley MG, Papadopoulos V. Structural and functional evolution of the translocator protein (18 kDa). *Curr Mol Med*. 2012;12(4):369–86.
43. Terada T, Yokokura M, Yoshikawa E, Futatsubashi M, Kono S, Konishi T, Miyajima H, Hashizume T, Ouchi Y. "Extrastriatal spreading of microglial activation in Parkinson's disease: a positron emission tomography study," *Annals of Nuclear Medicine* 2016;30(8):579–87.
44. Setiawan E, Wilson AA, Mizrahi R, Rusjan PM, Miller L, Rajkowska G, Suridjan I, Kennedy JL, Rekkas PV, Houle S, Meyer JH. Role of translocator protein density, a marker of neuroinflammation, in the brain during major depressive episodes. *JAMA Psychiat*. 2015;72(3):268–75.
45. Suridjan I, Pollock BG, Verhoeff NP, Voineskos AN, Chow T, Rusjan PM, Lobaugh NJ, Houle S, Mulsant BH, Mizrahi R. In-vivo imaging of grey and white matter neuroinflammation in Alzheimer's disease: a positron emission tomography study with a novel radioligand, [18F]-FEPPA. *Mol Psychiatry*. 2015;20(12):1579–87.
46. Suridjan I, Rusjan PM, Voineskos AN, Selvanathan T, Setiawan E, Strafella AP, Wilson AA, Meyer JH, Houle S, Mizrahi R. Neuroinflammation in healthy aging: a PET study using a novel Translocator Protein 18 kDa (TSPO) radioligand, [(18F)-FEPPA. *Neuroimage*. 2014;84:868–75.

Submit your next manuscript to BioMed Central and we will help you at every step:

- We accept pre-submission inquiries
- Our selector tool helps you to find the most relevant journal
- We provide round the clock customer support
- Convenient online submission
- Thorough peer review
- Inclusion in PubMed and all major indexing services
- Maximum visibility for your research

Submit your manuscript at  
[www.biomedcentral.com/submit](http://www.biomedcentral.com/submit)

